Jestr Journal of Engineering Science and Technology Review 8 (6) (2015) 44 – 48
Special Issue on Simulation of Manufacturing Technologies

JOURNAL OF
Engineering Science and Technology Review

www.jestr.org

Conference Article

2D Linear Friction Weld Modelling of a Ti-6Al-4V T-Joint

L. A. Lee[1,2]*, A. R. McAndrew[1], C. Buhr[1], K. A. Beamish[3] and P. A. Colegrove[1]

[1] *Welding Engineering and Laser Processing Centre (WELPC), Cranfield University, Cranfield, Bedfordshire MK43 0AL, U.K.*
[2] *National Structural Integrity Research Centre (NSIRC Ltd.), Granta Park, Great Abington, Cambridge, CB21 6AL, U.K.*
[3] *TWI Ltd, Granta Park, Great Abington, Cambridge CB21 6AL, U.K.*

Received 1 September 2015; Accepted 11 September 2015

Abstract

Most examples of linear friction weld process models have focused on joining two identically shaped workpieces. This article reports on the development of a 2D model, using the DEFORM finite element package, to investigate the joining of a rectangular Ti-6Al-4V workpiece to a plate of the same material. The work focuses on how this geometry affects the material flow, thermal fields and interface contaminant removal. The results showed that the material flow and thermal fields were not even across the two workpieces. This resulted in more material expulsion being required to remove the interface contaminants from the weld line when compared to joining two identically shaped workpieces. The model also showed that the flash curves away from the weld due to the rectangular upstand "burrowing" into the base plate. Understanding these critical relationships between the geometry and process outputs is crucial for further industrial implementation of the LFW process.

Keywords: Linear friction welding, finite element analysis, titanium, additive manufacture, material flow, flash formation, contaminant removal, thermal analysis.

1. Introduction

Linear friction welding (LFW) is a solid-state joining process that works by oscillating one workpiece relative to another whilst under a compressive force, as shown in Fig. 1. Despite being one continuous process, Vairis and Frost [1] noticed that LFW occurs over four phases:

- Phase 1 – the initial phase. The asperities on the surfaces to be joined interact and generate heat due to friction. The asperities soften and deform, increasing the true area of contact between the workpieces. Negligible axial shortening (burn-off) in the direction of the compressive force is observed.
- Phase 2 – the transition phase. The material plasticises and becomes viscous, causing the true area of contact between the workpieces to increase to 100 percent of the apparent cross-sectional area. Heat conducts back from the interface, plasticising more material, and the burn-off begins to occur due to the expulsion of the viscous material, forming the flash.
- Phase 3 – the equilibrium phase. The interface force, thermal profile and burn-off rate reach a quasi-steady-state condition and significant burn-off occurs through the rapid expulsion of the viscous material from the interface. The majority of the flash is generated during this phase.
- Phase 4 – the deceleration and forging phase. Once the desired burn-off is reached, the relative motion is ceased and the workpieces are aligned. In some applications an additional forging force may be applied to aid consolidation.

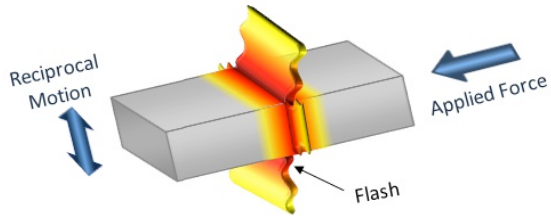

Fig. 1. An illustration of the LFW process.

Components machined from a solid block are often expensive due to the proportionally large amount of material that is purchased compared to the amount that remains after machining. LFW reduces the material required to make a component by joining smaller workpieces to produce a preform, which is subsequently machined to the desired dimensions. Currently, LFW is an established technology for the manufacture of titanium alloy integrated bladed disks (blisks) for aero-engines [2]–[6]. However, it is finding increasing interest from other industrial sectors – particularly for the joining of Ti-6Al-4V – due to the significant cost savings that can be achieved [3], [4], [7]. Despite the increased interest, the process has experienced limited additional industrial implementation [8], [9]. This is partly due to a lack of fundamental scientific understanding of LFW [8].

* E-mail address: lucie.lee@cranfield.ac.uk
ISSN: 1791-2377

Computational modelling offers a pragmatic method for understanding what is happening during the rapidly evolving process, allowing for increased fundamental scientific understanding [10]–[16]. An increased understanding will aid further industrial development and implementation of LFW.

To date, much of the research into LFW has been concerned with the joining of workpieces with identical surface contacting dimensions [1], [10]–[17]. There is an industrial interest to understand the joining of dissimilar sized workpieces. To address this, the present article reports on the development of a 2D finite element model to investigate the linear friction welding of a Ti-6Al-4V T-Joint.

2. Methodology: Development of a Model

This study uses the finite element analysis (FEA) software DEFORM to run a 2D model of a T-joint, the dimensions of interest for this study are shown in Fig. 2.

Based on the work by Turner et al. [16] and McAndrew et al. [14] the process was modelled as two distinct stages. The first stage used a purely thermal model to account for the heating during Phase 1 of the process and the second stage used a plastic flow model to account for the material flow during Phases 2 and 3. A single body was used to account for the material flow during Phases 2 and 3. The single body approach works on the principle that once the workpieces merge (Phase 2 onward) there is 100 percent true interfacial surface contact, thus allowing the process to be represented by a single body. To account for the earlier process heating a thermal profile must be mapped onto the model. This is vital as it allows the interface material of the single body model to deform in preference to its surroundings, as occurs in reality. The major benefit of the single body approach is that it enables the adhesion and mechanical mixing of the faying surfaces to be modelled, providing a better insight into flash formation and morphology [14], [16], [18].

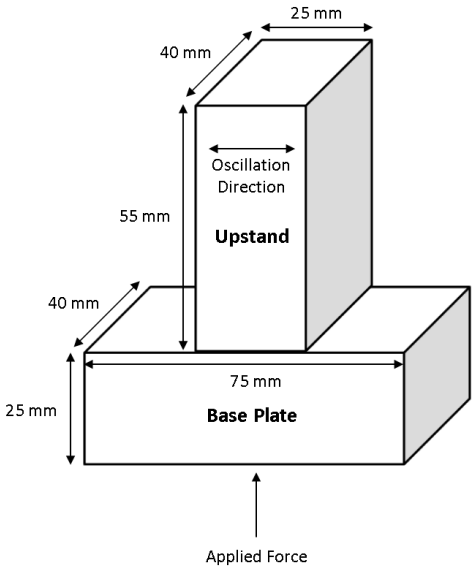

Fig. 2. Workpiece dimensions

2.1 Thermal Model

Previous work by McAndrew et al. [15] showed that, regardless of the process parameters used, the interface temperature reaches approximately 1000 °C at the end of the first phase at which point the flash formation occurs. A generic thermal profile that meets this requirement was developed using a similar approach to one reported elsewhere [15] and is shown in Fig. 3 (b). This thermal profile was used to provide the initial thermal condition for the single body model.

2.2 Plastic Flow Model

The single body model uses a 2D plane strain condition to represent the central slice of the workpieces shown in Fig. 2 along a plane parallel to the direction of oscillation. The reciprocal motion was generated by the oscillating tool die while the applied force was produced by the forging tool die, as shown in Fig. 3 (a). The stick-out from the tooling was 5 mm for each workpiece. The aforementioned thermal model was then mapped onto this plastic flow model, as shown in Fig. 3 (b). By definition, 2D analysis does not account for out-of plane material flow; despite this good predictive insights are still maintained [14], [16], [18].

The majority of the heat generation and plastic deformation throughout the process occurs along the weld interface. Based on the work by Turner et al. [16], an average mesh element size of 0.25 mm was used within an 8 mm band focused around this region. The relative element size was then increased with increasing distance from the weld line.

The accuracy of a plastic flow model is determined by input flow data. To avoid any inaccuracies due to data extrapolation, the material flow stress data for this model was the same as previously reported by Turner et al. [16] which covered the range of temperatures typically experienced during LFW. The material flow stress data was obtained from stress and strain curves for temperatures, strains and strain rates of 1500 °C, 4 and 1000 s^{-1} respectively. Tabular based temperature dependent thermal conductivity, specific heat and emissivity data from the DEFORM software's library were used. The temperature of the environment was assumed to be 20 °C.

A time-step of 0.0002 s was chosen to ensure that approximately one third of the weld line mesh element thickness was travelled per iteration. The model was thermo-mechanically coupled and it was assumed that 90% of the mechanical energy required for the material deformation was converted into heat [13,14]. The process parameters used for the model are shown in Table 1. The target burn-off of 3.25 mm was chosen because this was the maximum achievable burn-off for the current configuration while preventing the tooling from penetrating the flash.

Table 1. LFW parameters used for the model

Frequency of oscillation (Hz)	**Amplitude of oscillation** (mm)	**Applied force** (kN)	**Burn-off** (mm)
50	2	100	3.25

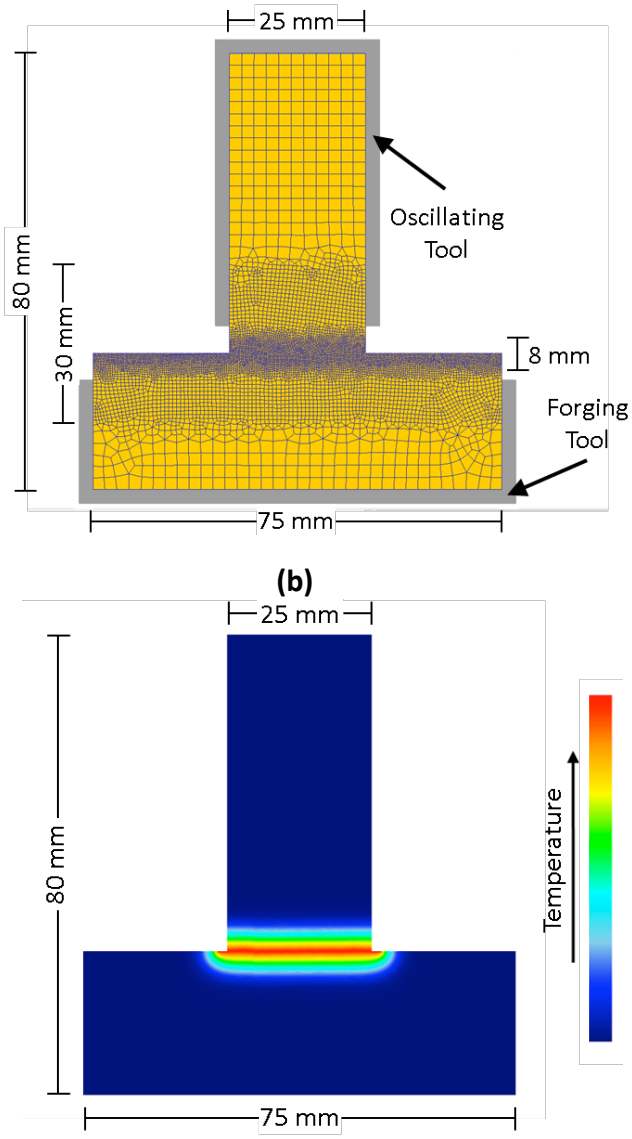

Fig. 3. Development of the 2D model including (a) the setup of the plastic flow model and (b) the thermal profile mapped onto the plastic flow model.

The model was used to study various thermal outputs of the process, including: the thermal profile, temperature gradient across the weld interface and the peak interface temperature. The flow of material at the interface was also investigated; this included the steady state burn-off rate, the peak strain rate, the expulsion of surface contaminants via point tracking, and the mechanism behind the flash formation.

3. Results and Discussion

3.1 Flash Formation and Material Flow

The modelled axial shortening (burn-off), recorded from the model, as shown in Fig. 4, was relatively linear. This is typical of the LFW process during Phase 3 due to a quasi-steady state condition being achieved. By measuring the gradient of the burn-off, a rate of 3.67 ± 0.04 mm.s^{-1} was obtained, which is in the same region recorded by other authors for a comparable set of process parameters [14].

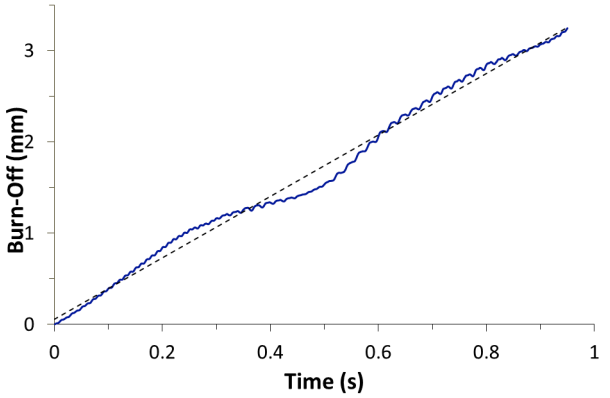

Fig. 4. Predicted burn-off (solid blue line) as a function of time where the burn-off rate is determined by the gradient of the curve (dashed black line), i.e. the linear line of best fit.

An investigation into the flash forming mechanism was conducted, as illustrated in Fig. 5. The model revealed that over the course of an oscillation, the flash remains attached to the upstand while it separates from the plate. The model predicted a maximum strain rate of over 1000 s^{-1} at the separation point when the upstand travelled away from the datum position, which was two times greater than the values recorded across the rest of the weld interface (500 s^{-1}). This large strain rate between the flash and the plate resulted in localised yielding of the material, hence the separation.

During the second half of the oscillation cycle, where the upstand returned to its original position, it was noticed that there was uneven expulsion of the plasticised material from the weld interface. The material across the upstand appeared to flow freely, while the material at the centre of the interface on the base plate side was restricted in its ability to flow. Interestingly, extra material toward the edges of the

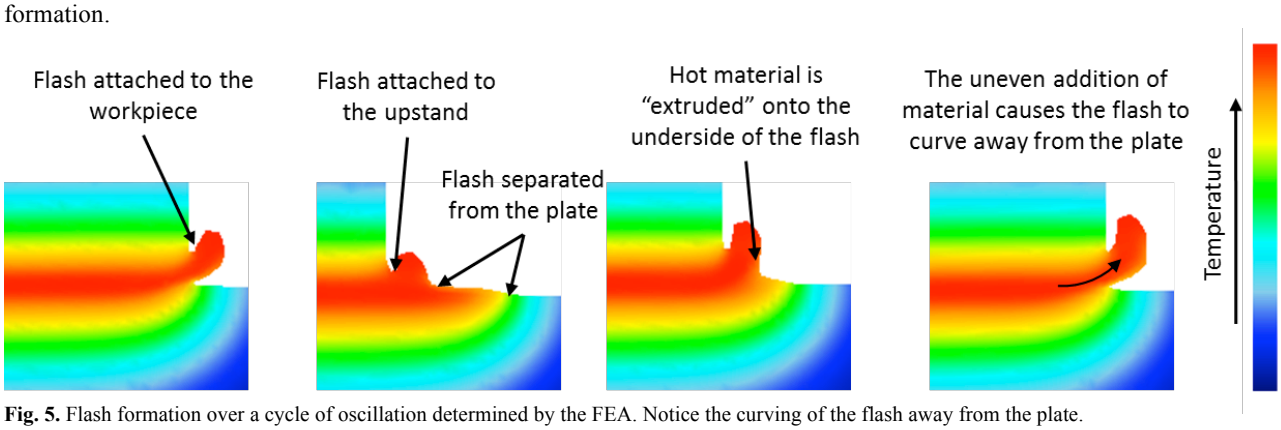

Fig. 5. Flash formation over a cycle of oscillation determined by the FEA. Notice the curving of the flash away from the plate.

weld on the base plate side was "scooped" out of the plate onto the underside of the flash, as shown in Fig. 5. This resulted in the upstand "burrowing" into the plate and caused the flash to curve away from the plate. The burrowing effect may explain why the material at the centre of the base plate did not flow as easily, the concave-like deformation profile in the base plate caused it to be held in place.

3.2 Surface Contaminant Removal

The removal of surface contaminants was studied by using point tracking along the interface, similar to the work reported by Turner et al. [16] and McAndrew et al. [14]. Each point was separated by a distance of 2 mm as illustrated in Fig. 6 (a).

Throughout the evolution of the weld, the gradual expulsion of the tracked points is observed. As shown in Fig. 6 (b), the model predicted that for the T-joint configuration not all of the point tracking were removed from the interface for the target burn-off of 3.25 mm. This is much more than the minimum required burn-off for complete contaminant removal for symmetric weld geometries [14]. This observation may be due to the burrowing effect. The tracked points may have been forced into the base plate material instead of being allowed to freely flow into the flash. This result highlights the importance of understanding the effects of the workpiece geometry on the material flow behavior of linear friction welds, something which is currently not well understood.

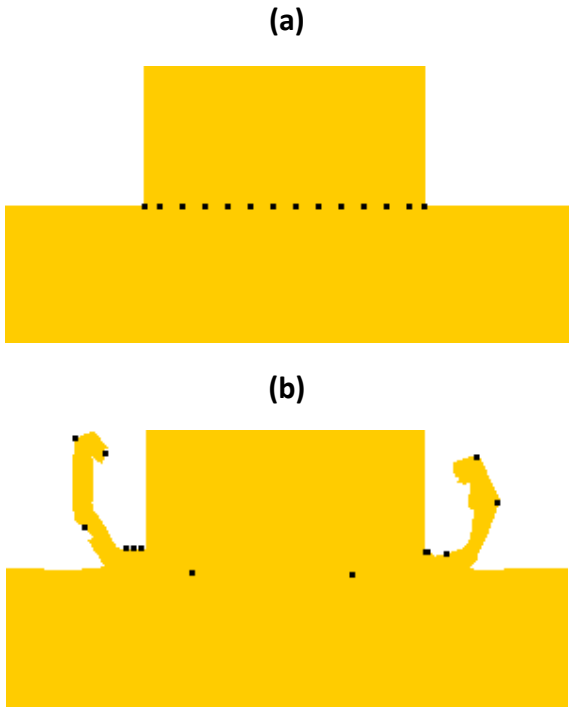

Fig. 6. Removal of surface contaminants around the weld line using interface point tracking: (a) initial location of the point tracking and (b) evolution of the point tracking.

3.3 Thermal Profile Evolution

The thermal profile across the centre of the interface was studied throughout the evolution of the process, as shown in Fig. 7 (a). A maximum temperature of approximately 1100°C was recorded at the interface, which is a comparable value to that reported for other Ti-6Al-4V linear friction welds [14], [16], [18]. The temperature then rapidly decreased away from the weld line. Despite the relatively low thermal conductivity of titanium, the spreading of the thermal profile with time demonstrates how the heat begins to soak into the surrounding workpieces throughout the process.

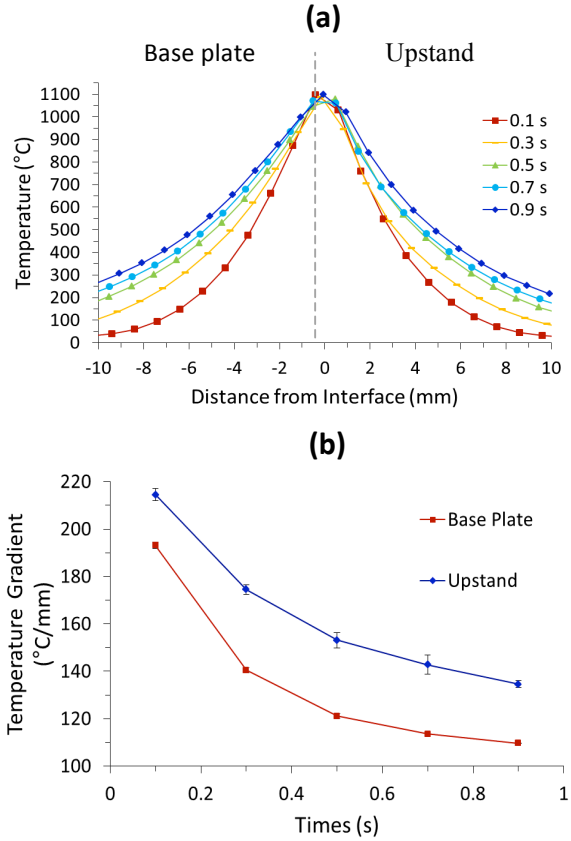

Fig. 7. Thermal fields across the weld interface throughout phase 3, showing (a) the temperature profile across the interface for different times throughout the equilibrium phase and (b) the magnitude of the temperature gradient either side of the interface as a function of time.

The temperature gradient between the weld interface and the region 3 mm back from the interface was recorded as a function of time and is shown in Fig. 7 (b). The results reveal a higher thermal gradient for the upstand than for the base plate. This is explained by the observed imbalance in expulsion of the hot plasticised material where the majority of material expelled appears to originate from the upstand, resulting in a steeper thermal gradient on this side. As discussed previously, the hot material at the centre of the weld on the base plate side remained at the weld interface for longer due to the difficulty in expelling it. This resulted in the heat building up in the base plate causing a wider thermal field, and hence, a shallower thermal gradient. The maximum thermal gradient recorded in the upstand was 215 ± 3 °C.mm^{-1}.

4. Conclusions

This paper presented the results of an initial investigation into the 2D FEA of a Ti-6Al-4V linear friction weld in the T-joint configuration. The following conclusions can be made from this work:

- The 2D model provided a novel insight into the LFW process for the joining asymmetrical Ti-6Al-4V workpieces.
- The material flow and thermal fields were not even across the two workpieces. This resulted in uneven expulsion of the plasticised material from the weld interface. The material across the rectangular upstand appeared to flow freely, while the material at the centre of the interface on the base plate side was restricted in its ability to flow.
- The rectangular upstand "burrowed" into the base plate.
- When compared to the literature on symmetrical workpieces, the surface contaminants did not flow into the flash as easily.
- The weld interface reached 1100 °C, surpassing the beta-transus temperature for this alloy.
- The gradient of the thermal profile was larger on the upstand-side than base plate-side.

5. Future Work

Future work by the authors will expand upon the modelling approach presented in this article to investigate the effects of the process parameters and workpiece orientation on Ti-6Al-4V T-joint linear friction welds. In addition, the modelling work will be experimentally validated to add further confidence to the results.

6. Acknowledgements

The authors would like to thank the Engineering and Physical Sciences Research Council (EPSRC) and The Welding Institute (TWI Ltd.) for funding the research presented in this paper. Also, the authors are very grateful to Dr. Alexander Bikmeyev of Ufa State Aviation Technical University, Russia for inviting us to present this work at SiMaTech-2015.

References

[1] A. Vairis and M. Frost, "High frequency linear friction welding of a titanium alloy," *Wear*, vol. 217, no. 1, pp. 117–131, 1998.
[2] Y. Guo, T. Jung, Y. Lung, H. Li, S. Bray, and P. Bowen, "Microstructure and microhardness of Ti6246 linear friction weld," *Mater. Sci. Eng. A*, vol. 562, pp. 17–24, 2013.
[3] I. Bhamji, M. Preuss, P. L. Threadgill, and A. C. Addison, "Solid state joining of metals by linear friction welding: a literature review," *Mater. Sci. Technol.*, vol. 27, no. 1, pp. 2–12, Jan. 2011.
[4] A. C. Addison, "Linear friction welding of engineering metals. TWI industrial members report - 894/2008," Cambridge, U.K., 2008.
[5] M. Karadge, M. Preuss, C. Lovell, P. J. Withers, and S. Bray, "Texture development in Ti–6Al–4V linear friction welds," *Mater. Sci. Eng. A*, vol. 459, no. 1–2, pp. 182–191, Jun. 2007.
[6] Y. Guo, Y. Chiu, M. Attallah, and H. Li, "Characterization of dissimilar linear friction welds of alpha + beta titanium alloys," *J. Mater. Eng. Perform.*, vol. 21, no. 5, pp. 770–776, 2012.
[7] A. C. Addison, "Linear friction welding information for production engineering. TWI industrial members report - 961/2010," Cambridge, U.K., 2010.
[8] W. Li, J. Suo, T. Ma, Y. Feng, and K. Kim, "Abnormal microstructure in the weld zone of linear friction welded Ti-6.5Al-3.5Mo-1.5Zr-0.3Si titanium alloy joint and its influence on joint properties," *Mater. Sci. Eng. A*, vol. 599, pp. 38–45, 2014.
[9] A. M. M. García, "BLISK fabrication by linear friction welding," in *Advances in Gas Turbine Technology*, E. Benini, Ed. Winchester: InTech, 2011, pp. 411–434.
[10] A. Vairis and M. Frost, "Modelling the linear friction welding of titanium blocks," *Mater. Sci. Eng. A*, vol. 292, no. 1, pp. 8–17, Nov. 2000.
[11] W. Li, S. X. Shi, F. F. Wang, T. J. Ma, J. L. Li, D. L. Gao, and A. Vairis, "Heat reflux in flash and its effect on joint temperature history during linear friction welding of steel," *Int. J. Therm. Sci.*, vol. 67, pp. 192–199, 2013.
[12] W. Li, F. Wang, S. Shi, T. Ma, J. Li, and A. Vairis, "3D finite element analysis of the effect of process parameters on linear friction welding of mild steel," *J. Mater. Eng. Perform.*, vol. 23, no. 11, pp. 4010–4018, Aug. 2014.
[13] W. Li, T. Ma, and J. Li, "Numerical simulation of linear friction welding of titanium alloy: Effects of processing parameters," *Mater. Des.*, vol. 31, no. 3, pp. 1497–1507, Mar. 2010.
[14] A. R. McAndrew, P. A. Colegrove, A. C. Addison, B. C. D. Flipo, and M. J. Russell, "Modelling the influence of the process inputs on the removal of surface contaminants from Ti-6Al-4V linear friction welds," *Mater. Des.*, vol. 66, pp. 183–195, 2015.
[15] A. R. McAndrew, P. A. Colegrove, A. C. Addison, B. C. D. Flipo, and M. J. Russell, "Energy and force analysis of Ti-6Al-4V linear friction welds for computational modeling input and validation data," *Metall. Mater. Trans. A*, vol. 45, no. 13, pp. 6118–6128, 2014.
[16] R. Turner, J.-C. Gebelin, R. M. Ward, and R. C. Reed, "Linear friction welding of Ti-6Al-4V: Modelling and validation," *Acta Mater.*, vol. 59, no. 10, pp. 3792–3803, Jun. 2011.
[17] U. U. Ofem, P. A. Colegrove, A. Addison, and M. J. Russell, "Energy and force analysis of linear friction welds in medium carbon steel," *Sci. Technol. Weld. Join.*, vol. 15, no. 6, pp. 479–485, Aug. 2010.
[18] F. Schröder, R. M. Ward, A. R. Walpole, R. P. Turner, M. M. Attallah, J.-C. Gebelin, and R. C. Reed, "Linear friction welding of Ti6Al4V: experiments and modelling," *Mater. Sci. Technol.*, vol. 31, no. 3, pp. 372–384, Feb. 2015.